Carbohydrate Polymers 332 (2024) 121885

Contents lists available at ScienceDirect

Carbohydrate Polymers

journal homepage: www.elsevier.com/locate/carbpol

Regioselective and controlled-density branching in amylose esters

Jeffrey E. Thompson [a], Kevin J. Edgar [a,b,*]

[a] Macromolecules Innovation Institute, Virginia Tech, Blacksburg, VA 24061, United States
[b] Department of Sustainable Biomaterials, Virginia Tech, Blacksburg, VA 24061, United States

A B S T R A C T

Herein, we report creation of methodology for one-pot synthesis of 2,3-*O*-acetyl-6-bromo-6-deoxy (2,3Ac-6Br) amylose with controlled degree of substitution of bromide (DS(Br)) followed by quantitative azide substitution as a route to branched polysaccharide derivatives. This methodology affords complete control of "tine" location, and strong control of degree of branching of comb-structured polymers. In this way, we achieved bromination strictly at C6 and esterification at the other hydroxy groups, where the DS(Br) at C6 was well-controlled by bromination/acylation conditions in the one-pot process. Azide displacement of all C6 bromides followed by copper-catalyzed azide-alkyne cycloaddition (CuAAC) click reaction with the small molecule *tert*-butyl propargyl ether (TBPE) demonstrated the potential to create such branched structures. This synthetic method has broad potential to generate well-defined polysaccharide-based comb-like structures, with a degree of structural control that is very unusual in polysaccharide chemistry.

1. Introduction

Polysaccharides are among the most abundant renewable natural polymers on Earth. Polysaccharides and their derivatives play pivotal roles in society including as drug delivery components, biodegradable films, viscosity modifiers, and renewable materials (Karan, Funk, Grabert, Oey, & Hankamer, 2019). Amylose is a particularly abundant polysaccharide, as the minor component of most starches. It comprises D-glucopyranose repeat units connected linearly via α 1 → 4 glycosidic linkages with minimal α 1 → 6 branching (Seung, 2020). Due to its isomerism with the structural polysaccharide cellulose (differing only in the stereochemistry of anomeric linkages), its natural abundance, and the plethora of possible chemical modifications of hydroxy groups to affect physical properties, amylose is an appealing candidate for high-value materials, particularly in biodegradable packaging. The physicochemical properties of polysaccharide derivatives depend not only on the nature and quantity of substituents, but also where they are appended to the anhydroglucose unit (AGU). As a result, there is tremendous interest in generating well-defined amylose derivatives with a high degree of substituent regioselectivity to better elucidate structure-property relationships.

A common method to append a wide variety of substituents to polysaccharides is via "click" chemistry, most notably the copper-catalyzed azide-alkyne cycloaddition (CuAAC). Independently reported by Meldal (Tornøe, Christensen, & Meldal, 2002) and Sharpless (Rostovtsev, Green, Fokin, & Sharpless, 2002), the CuAAC reaction is a Huisgen cyclcoaddition between an organic azide and terminal alkyne to generate a 1,4-disubstituted triazole (Huisgen, 1961). CuAAC exhibits the key features of "click" reactions: it is facile, high-yielding, tolerant to many conditions, generates no by-products, and is generally insensitive to the presence of other functional groups (Meng & Edgar, 2016). Polysaccharides can be imbued with functionality suitable for CuAAC either through incorporation of alkynyl or azido moieties. Previously described routes to incorporate alkyne groups include periodate oxidation followed by reductive amination with propargylamine (Bertoldo, Zampano, La Terra, Villari, & Castelvetro, 2011), esterification with an alkyne-terminated carboxylic acid (Kinose, Sakakibara, Ogawa, & Tsujii, 2019), or alkylation with propargyl halides (Pierre-Antoine, François, & Rachida, 2012). A single alkyne per polysaccharide chain can also be appended through reductive amination of the reducing end aldehyde moiety with propargylamine (Schatz, Louget, Le Meins, & Lecommandoux, 2009), which provides a route to polysaccharide-based block copolymers. Generally, azide moieties are appended to polysaccharides via the incorporation of a good leaving group, such as tosylate (Liebert, Hänsch, & Heinze, 2006) or halide (Yamashita, Okubo, Negishi, & Hasegawa, 2009) moieties, followed by S_N2 displacement with the azide anion. Azide functionality can also be incorporated at the reducing end through Lewis acid-catalyzed glycosylation with trimethylsilyl azide (Kamitakahara, Enomoto, Hasegawa, & Nakatsubo, 2005), which was employed to produce comb-like graft polymers with cellulosic side chains.

Regioselective synthesis of 6-azido-6-deoxyamylose has been investigated previously as a route to incorporate amine, amide, urea, and triazole moieties to generate functional amylose materials. Cimecioglu

* Corresponding author at: Department of Sustainable Biomaterials, Virginia Tech, Blacksburg, VA 24061, United States.
E-mail address: kjedgar@vt.edu (K.J. Edgar).

https://doi.org/10.1016/j.carbpol.2024.121885
Received 18 December 2023; Received in revised form 18 January 2024; Accepted 26 January 2024
Available online 4 February 2024

et al. reported the synthesis of 6-azido-6-deoxyamylose with DS(N_3) of 0.22, 0.37, and ~ 1.00 through regioselective halogenation either with triphenylphosphine (PPh_3) and *N*-bromosuccinimide (NBS) in *N,N*-dimethylacetamide (DMAc), or methanesulfonyl chloride (MsCl) in *N,N*-dimethylformamide (DMF) followed by azide substitution with sodium azide (NaN_3) in dimethyl sulfoxide (DMSO). The azide was subsequently converted to a primary amine through treatment either with lithium aluminum hydride ($LiAlH_4$) or by Staudinger reduction with PPh_3 (Cimecioglu, Ball, Kaplan, & Huang, 1994). Cimecioglu et al. later reported one-pot synthesis of 6-azido-6-deoxyamylose through treatment with PPh_3 and carbon tetrabromide (CBr_4) in a DMF/lithium azide (LiN_3) solvent system (Cimecioglu, Ball, Huang, & Kaplan, 1997); although not isolated, it is believed that a 6-bromo-6-deoxyamylose intermediate was formed in situ at the C6-position before azide displacement. It should also be noted that the authors observed that an excess of PPh_3 could react with the C6-N_3 to generate an iminophosphorane which could be hydrolyzed to a primary amine upon aqueous workup. The more stable NaN_3 can be substituted for LiN_3 to generate 6-azido-6-deoxyamylose and 6-azido-6-deoxyamylopectin as precursors to photochromic materials (Barsi et al., 2017). Zhang et al. employed the MsCl/DMF method to generate 6-azido-6-deoxyamylose with DS(N_3) 0.98, which was subsequently reduced to the amine with sodium borohydride ($NaBH_4$) and benzoylated to generate 6-benzamido-6-deoxyamylose (Zhang et al., 2020). However, to our knowledge, there have been no attempts to generate *O*-acylated 6-azido-6-deoxyamylose, which is expected to be a valuable precursor to CuAAC-functional polysaccharides, to do so in a one-pot process, or to develop methods in that one-pot process to precisely control the degree of bromination and subsequent azide displacement, which will control degree of branching and thus heavily influence properties.

Previous investigators have shown the value of Furuhata bromination for selective functionalization of polysaccharides that contain a C6-OH group. In turn, azide displacement of that C6-Br is typically quantitative, and the azide can be a precursor to a menu of *N*-containing functional groups. Thus, it is possible, with virtually complete regioselectivity, to append an azide moiety to the C6-position of cellulose (Fox & Edgar, 2012), curdlan (Zhang & Edgar, 2014), or pullulan (Pereira & Edgar, 2014). From these C6-N_3 polysaccharides, one can generate regioselectively peracylated derivatives containing amides, primary amines, secondary amines (Zhang, Liu, & Edgar, 2017) and ω-carboxyamides (Liu, Gao, Mosquera-Giraldo, Taylor, & Edgar, 2018), all regioselectively substituted at the C6-position. However, we have not yet investigated 6-azido-6-deoxy polysaccharides or their *O*-acylated counterparts as CuAAC functional materials, nor have we attempted to generate *O*-acylated 6-azido-6-deoxy polysaccharides with DS(N_3) much less than1.00.

Comb-like structures based on polysaccharides, where the polysaccharide comprises the graft polymer backbone, have gained increased attention as blend compatibilizers (Saadatmand, Edlund, & Albertsson, 2011), thermoplastic elastomers (Jiang, Wang, Qiao, Wang, & Tang, 2013), and internally-plasticized materials (Imre, Kiss, Domján Cui, & Pukánszky, 2021), all of which are valuable for sustainable plastics. We envision that regioselectively *O*-acylated-6-azido-6-deoxy polysaccharides with varying DS(N_3) could be valuable precursors to generate well-defined polysaccharide derivatives with functionality that permits CuAAC chemistry. These regioselectively substituted derivatives could provide a route to well-defined polysaccharide-based comb-structured polymers, and perhaps eventually comb-like graft polymers, allowing for elucidation of structure-property relationships between polymer performance and side chain density. By controlling DS(N_3) to synthesize graft polymers through grafting-to CuAAC with a pre-synthesized alkyne-terminated polymer, a route can be established to generate well-defined polysaccharide-based graft polymers with precise control over the grafting density and molecular weight of the graft polymer side chain. Carrying out this transformation as a one-pot process would not only be efficient; it would avoid the complexities inherent in the poor solubilities typically observed for 6-(azido or halo)-6-deoxy polysaccharide derivatives. On the other hand, targeting DS of C6-Br less than one becomes quite complicated in a one-pot process; it sets up the possibility of competition between acylation and bromination at C6, which must be well-controlled in order to reach target "tine" density.

The goal of the current study is to develop a one-pot acylation/bromination procedure to generate fully substituted amylose derivatives with varying DS(6-Br), allowing for two-step preparation of regioselectively *O*-acylated 6-azido-6-deoxyamyloses with varying DS(6-N_3). We hypothesize that the density of C6-Br of functionalized amylose prepared by one-pot acylation/bromination reaction can be controlled by varying stoichiometry, order of addition, and reaction times. To our knowledge, this is the first reported approach to one-pot synthesis of 2,3Ac-6Br amylose, and the first employment of one-pot bromination/acylation in an attempt to generate persubstituted amylose derivatives with varying DS(Br) and DS(Ac). We expect that this control over functionalization density of fully substituted amylose esters can provide a pathway to well-defined polysaccharide-based comb-structured graft polymers with precise control over branch location and density, allowing in-depth structure-property relationship studies.

2. Experimental

2.1. Materials

Amylose isolated from potato starch (Biosynth, YA10257), with M_n = 1610 kg/mol (degree of polymerization (DP_n) = 9940) and $Đ$ = 4.12 (determined from size exclusion chromatography (SEC) of its tricarbanilate derivative), was dried at 50 °C under reduced pressure overnight before use. *N,N*-Dimethylacetamide (DMAc, Fisher), dimethyl sulfoxide (DMSO, Sigma), *N,N*-dimethylformamide (DMF, Spectrum), and pyridine (Sigma) were stored over 4Å molecular sieves. LiBr (Alfa Aesar) and NaN_3 (Fisher) were dried overnight at 125 °C under reduced pressure and stored in a desiccator under vacuum until use. PPh_3 (Sigma) was recrystallized from ethanol (EtOH) and dried at room temperature (RT) under reduced pressure for 2 days. NBS (Acros) was recrystallized from boiling water and dried at RT over anhydrous $CaCl_2$ under reduced pressure for 2 days. Acetic anhydride (Ac_2O, Acros), copper(I) bromide (Oakwood Chemical), *tert*-butyl propargyl ether (TBPE, Alfa Aesar), *N,N,N',N'',N''*-pentamethyldiethylenetriamine (PMDETA, Oakwood Chemical), and phenyl isocyanate (Acros) were used as received. Regenerated cellulose dialysis tubing (3.5 kDa MWCO, Spectrum) was soaked in deionized water for at least 30 min prior to use. All other solvents were of reagent grade and used as received.

2.2. Measurements

^1H, ^{13}C, quantitative ^{13}C ($q^{13}C$), and heteronuclear single quantum coherence (HSQC) NMR spectra were obtained on either a Bruker Avance II 500 MHz spectrometer equipped with a BBO Prodigy probe or a Bruker Avance III 600 MHz spectrometer equipped with a TCI Prodigy Probe at RT. Samples were dissolved in deuterated DMSO (DMSO-d_6), deuterated chloroform ($CDCl_3$), or 1:1 v:v DMSO-d_6:$CDCl_3$ depending on DS(Ac) and DS(C6-X). 2,3Ac-6Br amylose and 2,3Ac-6N_3 amylose were dissolved at approximately 80 mg/mL and 2,3Ac-6*t*Bu amylose was dissolved at approximately 10 mg/mL. ^1H NMR spectra were obtained with at least 64 scans with 1 s delay. ^{13}C NMR spectra were obtained using at least 2048 scans with 3 s delay. Quantitative ^{13}C NMR samples contained 0.025 M chromium(III) acetylacetonate ($Cr(Acac)_3$) and spectra were obtained using at least 2048 scans with 3 s delay. HSQC spectra were obtained using at least 8 scans with 512 increments with 2 s delay. Elemental analysis (EA) was performed by Midwest Microlab to determine C, H, and N contents by flask combustion followed by ion chromatography. Fourier transform infrared (FTIR) spectra were acquired using a Varian 670 IR spectrometer equipped with a Pike

Technologies GladiATR attachment and collected as the average of 32 scans. SEC was performed in DMAc with 50 mM LiCl at 25 °C at a flow rate of 0.5 mL/min (Agilent isocratic pump, degasser, and autosampler, columns: TOSOH TSKgel Guard Alpha and TOSOH TSKgel Alpha-3000: molecular weight range 0–1 × 10^5 g/mol). Detection consisted of a Wyatt Optilab refractive index (RI) detector operating at 785 nm, a Wyatt DAWN multi-angle light scattering detector operating at 783 nm, and an Agilent MWD operating at 365 nm. Absolute molecular weights and dispersities were calculated with the Wyatt ASTRA software and off-line dn/dc analysis, assuming 100% mass recovery. Thermogravimetric analysis (TGA) was performed using a TA Instruments TGA 5500 at a heating rate of 20 °C/min up to 500 °C. Glass transition temperatures (T_g) were obtained by differential scanning calorimetry (DSC) performed on a TA Instruments DSC Q2500. Samples were heated at 10 °C/min up to approximately 30–50 °C below onset of decomposition, then cooled at 20 °C/min to 0 °C, then heated again at 10 °C/min. T_g values were obtained from the second heating cycle to erase any previous thermal history. DSC experiments were performed in triplicate to obtain the average and standard deviation of T_g for each composition. DS values were obtained by EA, ^{1}H NMR, and/or q^{13}C NMR and calculated using the following equations:

$$(1)\ \mathrm{DS(Ac)} = \frac{7 \times \mathrm{I(Ac - CH_3)}}{3 \times \mathrm{I(backbone)}}$$

DS(Ac) is the DS of acetyl groups. I(Ac -CH_3) is the integral of acetyl methyl resonances and I(backbone) is the integral of amylose AGU backbone resonances, both obtained from ^{1}H NMR. There are 7 protons per amylose AGU and 3 protons per acetyl methyl group.

$$(2)\ \mathrm{DS(N_3)} = \frac{\mathrm{I(C6 - N_3)}}{\mathrm{I(C6 - N_3) + I(C6 - OAc)}}$$

$$(3)\ \mathrm{DS(N_3)} = \frac{\left(\frac{\%N}{3}\right) \times 12.011 \times (6 + (2 \times \mathrm{DS(Ac)}))}{\%C \times 14.007}$$

DS(N_3) is the DS of azide groups substituted at the 6-position. Azide substitution was observed to be quantitative, so it is assumed that DS(Br) = DS(N_3). I(C6-N_3) is the integral of C6 azide resonances and I(C6-OAc) is the integral of C6 acetyl resonances, both obtained from q^{13}C NMR. %N and %C are the weight fractions of nitrogen and carbon, respectively, obtained from EA.

$$(4)\ \mathrm{DS}(t\mathrm{Bu}) = \frac{7}{9}\left[\frac{\mathrm{I}(t\mathrm{Bu} - \mathrm{CH_3})}{\mathrm{I(backbone)} - \frac{2}{9}\mathrm{I}(t\mathrm{Bu} - \mathrm{CH_3})}\right]$$

DS(*t*Bu) is the DS of *tert*-butyl groups substituted at the 6-position. I(*t*Bu -CH_3) is the integral of *tert*-butyl methyl resonances. CuAAC was assumed to be quantitative, so it is assumed that DS(N_3) = DS(*t*Bu). Unfortunately, the resonances from the methylene protons from the TBPE moiety overlap with the AGU backbone resonance. However, the ratio between *tert*-butyl methyl and TBPE methylene protons is known, which allows for correction of the AGU backbone integral. There are 9 protons per *tert*-butyl group and 2 protons per TBPE methylene group.

2.3. Dissolution of amylose in DMAc/LiBr

This procedure was adapted from a previously published procedure (Edgar, Arnold, Blount, Lawniczak, & Lowman, 1995). In an oven-dried, N_2-flushed 500 mL 3-neck round-bottom flask equipped with N_2 inlet, mechanical stirrer, and short path distillation apparatus, dry amylose (2.50 g, 15.4 mmol AGU) was slurried in anhydrous DMAc (100 mL) under dry N_2 at 160 °C for 30 min. Dry LiBr (10.0 g, 115 mmol, 7.46 eq/AGU) was added followed by additional anhydrous DMAc (20 mL) and stirred for an additional 10 min at 160 °C. Approximately 20 mL of DMAc was distilled at 160 °C under slight vacuum to remove any adventitious water present. The flask was then backfilled with dry N_2 and allowed to cool to RT, resulting in a transparent, amber solution within 2 h. All solutions were kept under dry N_2 until use within 24 h.

2.4. Representative procedure for one-pot synthesis of 2,3Ac-6Br amylose

In two oven-dried 100 mL round-bottom flasks, NBS (2.74 g, 15.4 mmol, 1 eq/AGU) and PPh_3 (4.04 g, 15.4 mmol, 1 eq/AGU) were dissolved in separate portions of anhydrous DMAc (50 mL each). After all contents had dissolved, the PPh_3 solution was added to the amylose solution over 5 min, followed by the NBS solution, also added over 5 min, all under dry N_2. After all contents were added, the flask was lowered into an oil bath set at 70 °C. After 1 h, Ac_2O (14.6 mL, 154 mmol, 10 eq/AGU) was quickly added to the flask, the temperature was raised to 80 °C, and the solution stirred at that temperature under dry N_2 for 24 h. The solution was cooled to RT, then slowly added to 2.5 L chilled 1:1 deionized water:methanol (MeOH) to precipitate the product, which was isolated by filtration. The crude product was redissolved in a mixture of acetone and ethyl acetate (EtOAc), concentrated by rotary evaporation, then reprecipitated into EtOH. The product was isolated by filtration, redissolved, and reprecipitated again into EtOH. Finally, the product was collected by filtration and dried overnight at 50 °C under reduced pressure. All products were recovered at approximately 75% yield. ^{1}H NMR (500 MHz, $CDCl_3$): 1.95–2.01 (C2 & C3 Ac -C$\underline{H}_3$), 2.16–2.18 (C6 Ac -C$\underline{H}_3$) 3.67–3.77 (C6 -C$\underline{H}_2$-Br), 3.92–5.27 (C1-C5 -C$\underline{H}$), 4.22–4.53 (C6 -C$\underline{H}_2$-OAc). ^{13}C (125 MHz, $CDCl_3$): 20.6–21.0 (Ac -$\underline{C}H_3$), 33.7 (C6 -$\underline{C}H_2$-Br), 62.2 (C6 -$\underline{C}H_2$-OAc), 69.0–72.9 (C2-C5 -$\underline{C}$H), 95.7 (C1 -$\underline{C}$H), 169.6 (C6 -O$\underline{C}$OCH$_3$), 170.5–170.8 (C2 & C3 -O$\underline{C}$OCH$_3$).

2.5. Representative procedure for synthesis of 2,3Ac-6N_3 amylose

In an oven-dried 250 mL single-necked round-bottom flask, 2,3Ac-6Br amylose (DS(Ac) 2.73, DS(6-Br) 0.26, 2.50 g, 8.56 mmol AGU) was dissolved in anhydrous DMSO (100 mL) at 40 °C overnight. Once dissolved, NaN_3 (1.39 g, 2.5 eq/AGU) was added to the flask. The reaction solution was then heated to 80 °C and stirred at that temperature for 24 h. After 24 h, the solution was cooled to RT and slowly added to 1.5 L chilled MeOH. The product was isolated by filtration, redissolved in a mixture of acetone and EtOAc, concentrated by rotary evaporation, then reprecipitated into EtOH. The final product was collected by filtration and dried overnight at 50 °C under reduced pressure. It was difficult to find an effective non-solvent for 2,3Ac-6N_3 Amylose DS(Ac) 2.01 (water was an effective non-solvent except that precipitation into water afforded fine particles that were difficult to isolate by filtration), so after 24 h the reaction solution was cooled and poured directly into 3.5 kDa MWCO dialysis tubing prewet with water. The tubing was dialyzed against deionized water for 1d, MeOH for 1d, and 19:1 EtOH: acetone for 1d, after which the contents were removed, collected, washed by centrifugation with H_2O (3 × 30 min, 8000 RPM), and dried overnight at 50 °C under reduced pressure. All products were recovered at approximately 80% yield. ^{1}H NMR (500 MHz, $CDCl_3$): 1.94–2.01 (C2 & C3 Ac -C$\underline{H}_3$), 2.15–2.19 (C6 Ac -C$\underline{H}_3$), 3.50–3.62 (C6 -C$\underline{H}_2$-N_3), 3.85–5.37 (C1-C5 -C$\underline{H}$), 4.22–4.53 (C6 -C$\underline{H}_2$-OAc). ^{13}C NMR (125 MHz, $CDCl_3$): 20.6–21.0 (Ac -$\underline{C}H_3$), 51.2 (C6 -$\underline{C}H_2$-N_3), 62.2 (C6 -$\underline{C}H_2$-OAc), 69.0–72.9 (C2-C5 -$\underline{C}$H), 95.7 (C1 -$\underline{C}$H), 169.6 (C6 -O$\underline{C}$OCH$_3$), 170.5–170.8 (C2 & C3 -O$\underline{C}$OCH$_3$). Elemental analysis: C 48.96%, H 5.61%, N, 3.70%; theoretical DS(Ac) 2.73, DS(N_3) 0.27: C 49.79%, H 5.57%, N 4.00%.

2.6. Representative procedure for CuAAC of 2,3Ac-6N_3 amylose with TBPE

In an oven-dried, N_2-flushed 25 mL 3-neck flask equipped with a N_2 inlet and septum, 2,3Ac-6N_3 amylose (DS(Ac) 2.73, DS(6-N_3) 0.26, 100

mg, 0.35 mmol AGU) and TBPE (71.0 μL, 0.53 mmol, 1.5 eq/AGU) were dissolved in anhydrous DMF (4.5 mL) under dry N_2. Once dissolved, the solution was sparged with dry N_2 for 10 min. In a 1-dram vial equipped with a septum, Cu(I)Br (25.2 mg, 0.18 mmol, 0.5 eq/AGU) and PMDETA (36.8 μL, 0.18 mmol, 0.5 eq/AGU) were dissolved in anhydrous DMF (1 mL) and subsequently sparged with N_2 for 5 min. Then, 500 μL of the catalyst/ligand solution was added to the polymer solution under N_2 using an N_2-flushed syringe. The flask was then immersed in a 50 °C oil bath and stirred for 24 h at that temperature. After 24 h, the solution was cooled to RT, diluted with DMF, and passed repeatedly through a plug of basic alumina to remove Cu. The filtrate was collected, concentrated via rotary evaporation, then added to 40 mL EtOH to precipitate the product. The precipitate was washed by centrifugation with EtOH (3 × 30 min, 8000 rpm), isolated by filtration, collected, and dried overnight at 50 °C under reduced pressure. 2,3Ac-6tBu amylose DS(Ac) 2.01 was precipitated into deionized water and washed with 9:1 deionized water: MeOH due to its partial solubility in EtOH. All products were recovered at approximately 60% yield. ^{1}H NMR (600 MHz, 1:1 $CDCl_3$:DMSO-d_6): 1.19 (-O-C(CH_3)$_3$), 1.89–1.96 (C2 & C3 Ac -CH_3), 2.06–2.09 (C6 Ac -CH_3), 3.95–4.45 (C6 -CH_2-N-), 3.89–5.28 (C1-C5 -CH), 3.95–4.45 (C6 -CH_2-OAc), 4.36–4.48 (-C-CH_2-O-*t*Bu), 7.84 (triazole -N-CH=C-). ^{13}C NMR (150 MHz, 1:1 $CDCl_3$:DMSO-d_6): 20.1–21.3 (Ac -CH_3), 27.7 (*t*Bu -C(CH_3)$_3$), 49.6 (C6 -CH_2-N-), 55.4 (-C-CH_2-O-tBu), 63.1 (C6 -CH_2-OAc), 68.9–74.0 (C2-C5 -CH), 73.0 (-O-C(CH_3)$_3$), 95.6 (C1 -CH), 125.0 (triazole -N-CH=C-), 145.3 (triazole -N-CH=C-), 169.0 (C6 -OCOCH$_3$), 169.5–169.7 (C2 & C3 -OCOCH$_3$).

3. Results and discussion

3.1. One-pot Regioselective Bromination and acetylation of amylose in DMAc/LiBr: Synthesis of 2,3Ac-6Br amylose

To imbue amylose esters regioselectively with an azide moiety for future CuAAC modification, we first had to incorporate a good leaving group at the C6 position (See Scheme 1). We chose to employ the well-documented regioselective bromination of polysaccharide primary alcohols using NBS and PPh_3 (Furuhata, Koganei, Chang, Aoki, & Sakamoto, 1992) which is one of the most regiospecific halogenation reactions in polysaccharide chemistry (Fox, Li, Xu, & Edgar, 2011). Previous reports from our lab expanded on this work by subsequent addition of an acid anhydride to acylate remaining hydroxyl groups in situ without isolation of the 6-bromo-6-deoxy polysaccharide intermediate to directly generate fully, entirely regioselectively substituted derivatives, 2,3-*O*-acyl-6-bromo-6-deoxycellulose haloesters (Fox & Edgar, 2011; Marks, Fox, & Edgar, 2016).

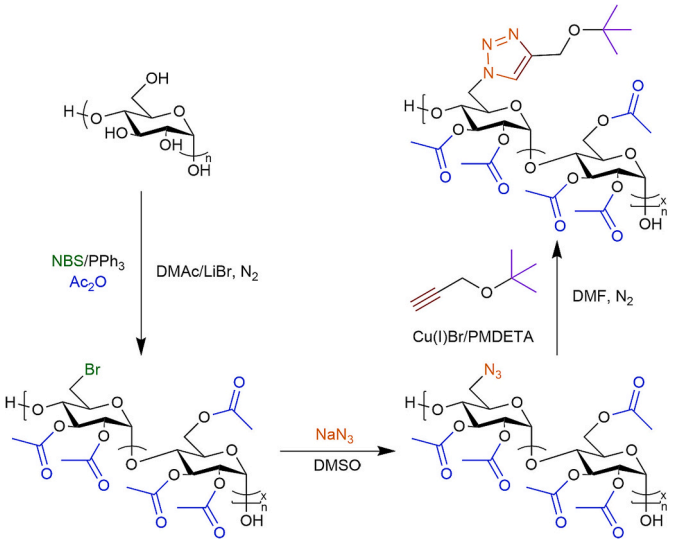

Scheme 1. Reaction scheme of one-pot regioselective bromination/acetylation of amylose, followed by azide substitution and CuAAC with TBPE.

In our first attempts to synthesize 2,3Ac-6Br amylose, we employed a catalytic amount of dimethylaminopyridine (DMAP) to catalyze acetylation of the remaining hydroxy groups. However, resonances associated with the aromatic ring and methyl groups of DMAP were still apparent in ^{1}H NMR spectra after workup and subsequent reactions (data not shown). This suggests that DMAP acted as a nucleophile and generated the dimethylaminopyridinium bromide salt at the C6 position; while undesired, this could provide a one-pot route to polysaccharide esters regioselectively substituted with cationic derivatives at the 6-position, which are materials that have shown promise for drug and gene delivery applications (Liu & Edgar, 2017; Liu, Liu, Esker, & Edgar, 2016; Marks et al., 2016). Subsequently, we did not employ any catalyst for acylation and achieved almost full substitution of hydroxyl groups, which is supported by the lack of -OH stretch absorption in FTIR spectra (see Supplementary Information).

While it seems simple on paper to carry out fully regioselective bromination followed by fairly facile acylation of the remaining -OH groups, with a high degree of regioselectivity and stoichiometric control, in practice (if one wishes to carry it out as a one-pot procedure) it is not so straightforward. Carrying out these transformations in one pot is not only convenient, relatively inexpensive, and efficient, but also avoids the problem of redissolving the intermediate, relatively poorly soluble 6-bromo-6-deoxyamylose derivative (which is even more challenging when targeting incomplete bromination at C6). Furuhata bromination is quite regioselective and can be carried out to high conversion (essentially quantitative, if desired), but requires an excess of NBS and PPh_3. Therefore, some unconsumed bromination reagent will still be present upon adding the acylating reagent in a one-pot process. What will be the result of the ensuing kinetic competition between C6 bromination and C6 acylation, and how can DS(acyl) and DS(6-Br) be controlled when simultaneous reactions are competing for C6-OH groups? It is important to answer these questions in order to be able to make amylose derivatives with a low incidence of "tines" along the comb-like structure. We anticipated that it would become even more important in later work, when we might wish to have tine incidence as low as 1 per 10 AGU to attain peak graft (co)polymer performance (Tsou et al., 2016; López-Barrón & Tsou, 2017; Kilmovica et al., 2020; Self et al., 2022). The ability to append bromide or azide to C-6 with essentially complete control of regioselectivity and strong control over DS will provide a number of handles directly or by simple modification (-Br, -N_3, -NH_2) that can be employed as electrophiles, nucleophiles, or cycloaddition partners for appending targeted substituents, including polymeric substituents.

We planned to vary DS(6-Br) by varying stoichiometric equivalents of NBS and PPh_3 per amylose AGU. It was observed that near-complete C6 bromination was obtained with 4 eq each of NBS/PPh_3 at 70 °C for 1 h, and subsequent esterification of the remaining 2,3- secondary hydroxyl groups was achieved by treatment with 10 eq per AGU of Ac_2O at 80 °C for 24 h, similar to our previous results for one-pot bromination and acylation of cellulose (Fox & Edgar, 2011). We observed DS(Ac) 2.01 under these conditions, indicating that all secondary hydroxyl groups and a small amount of primary hydroxyl groups was acetylated. Acetylation of the 6-position is a known side reaction of the NBS/PPh_3 bromination, where DMAc solvent acts as a nucleophile and attacks the C6 alkoxyphosphonium intermediate instead of a bromine anion (Furuhata et al., 1992). There were no resonances associated with aromatic signals in either ^{1}H or ^{13}C NMR spectra of all derivatives except for 2,3Ac-6Br amylose DS(Ac) 2.01, indicating that PPh_3 and triphenylphosphine oxide (PPh_3O) residues were effectively removed by two reprecipitations into EtOH. PPh_3 and PPh_3O are notoriously difficult impurities to remove from polysaccharides after NBS/PPh_3 bromination (Liu & Edgar, 2017).

The ratio of equivalents of NBS/PPh_3 per AGU had a significant effect

on DS(6-Br) and DS(Ac). As seen in Table 1, DS(Ac) increased with decreasing stoichiometric equivalents of NBS/PPh_3 per AGU, which we suggest was due to a decrease in DS(6-Br) in the allotted 1 h reaction time before Ac_2O addition. From the ^1H NMR spectra shown in Fig. 1, it was observed that 2,3Ac-6Br DS(Ac) 2.01 exhibited two broad singlet resonances between 1.89 and 2.02 ppm which was attributed to the C2,3-OAc groups and a small singlet resonance between 2.12 and 2.19 ppm which was attributed to C6-OAc groups. As DS(Ac) increased, the intensity of the C6-OAc resonance increased while the intensity of the C2,3-OAc remained constant, indicating that the increase in DS(Ac) is a result of increasing DS(Ac) at the C6 position. A similar trend was also observed in ^{13}C NMR spectra (see Supplementary Information). For 2,3Ac-6Br DS(Ac) 2.01, there existed resonances at 20.4–20.6, 35.2, and 169.6–170.0 ppm which are attributed to acetate methyl, C6-Br methylene, and acetate carbonyl carbons, respectively. As DS(Ac) increased, new resonances appeared at 20.3, 62.9, and 169.4 ppm which were attributed to C6-OAc methyl, C6-OAc methylene, and C6-OAc carbonyl groups, respectively. The ^1H and ^{13}C NMR chemical shifts for C1-C5 of the AGU ring were correlated and identified using HSQC NMR and were in good agreement with the chemical shifts previously reported for amylose acetate (Fringant, Desbrières, & Rinaudo, 1996) (See Supplementary Information). The highest DS(Ac) observed as we varied reaction stoichiometry was 2.73, which was obtained after treatment of amylose with 1 eq per AGU of NBS/PPh_3 for 1 h at 70 °C followed by 10 eq per AGU of Ac_2O for 24 h. This indicates that bromination was incomplete with 1 eq after 1 h at 70 °C; therefore, upon addition of the acetylating agent, it competed with NBS/PPh_3 for the remaining C6-OH groups.

Interestingly, no bromination was observed when using 0.5 or 0.75 equivalents of NBS/PPh_3 per AGU, and the products from those reactions were essentially amylose triacetate with DS(Ac) > 2.97 (data not provided). One could attribute this observation to the low concentration of brominating agents in solution, as first NBS and PPh_3 react to form a phosphonium salt which in turn is attacked by the C6-OH of amylose to generate an activated phosphonium ester. The bromine anion supplied by both NBS and LiBr can then attack the activated phosphonium ester via S_N2 displacement to generate a primary alkyl bromide (these sequential S_N2 displacements are the source of the near-perfect regioselectivity of Furuhata bromination of polysaccharides). The low concentration of both NBS and PPh_3 provides low collision frequency between the two, as well as between the C6-OH and the phosphonium salt generated in situ. However, the complete lack of observable bromination at these concentrations is still surprising. It cannot be ruled out that some reaction component or contaminant consumes some of the brominating reagents, leading to the requirement for fairly large excess; it is not immediately clear to us what that entity might be. A third alternative could be that the mechanism is more complex than has been previously thought, where PPh_3 and/or NBS react bimolecularly to form a stable intermediate, which is only converted to the 6-bromo-6-deoxy-polysaccharide after intervention of a second molecule of either (which would have to be a kinetically slower step). Again, the exact nature of such an alternative mechanism is unclear to us; in any case, these results with less than one equivalent of each reagent constitute an intriguing clue that the full mechanistic details of this valuable bromination may not yet be understood.

Table 1
Results of one-pot bromination/acetylation of amylose in DMAc/LiBr.

Entry	NBS/PPh_3: AGU	t(h) @ RT	t(min) @ 70 °C	t(h) @ 80 °C	DS (Ac)
Series 1: Effect of NBS/PPh_3:AGU on DS(Ac)					
A	4:1	0	60	24	2.01
B	2:1	0	60	24	2.64
C	1.5:1	0	60	24	2.67
D	1:1	0	60	24	2.73
Series 2: Effect of bromination time at 70 °C on DS(Ac)					
E	1:1	0	30	28	2.81
F	1:1	0	10	32	2.71
G	1:1	0	3	32	2.68
Series 3: Effect of addition of Ac_2O at RT before adding NBS/PPh_3 on DS(Ac)					
H	1:1	1	60	32	2.88
I	1:1	2	60	32	2.96

We then sought to investigate the effect of bromination reaction time prior to Ac_2O addition on DS(Br) and DS(Ac). We envisioned that earlier addition of Ac_2O would compete with bromination, resulting in more acetylation of primary hydroxyl groups and preventing further increase in DS(6-Br). Interestingly, DS(Ac) decreased as we decreased the time during which only brominating agent was present (at 70 °C) before adding Ac_2O and increasing to 80 °C. The lowest DS(Ac) observed was 2.68 (with DS(6-Br) 0.25) when only brominating agent was present for 3 min before Ac_2O addition and temperature increase. We believe it is likely that the earlier increase of reaction temperature accelerated bromination rate more than it did the acetylation kinetics.

After it was apparent that changing stoichiometry and reaction times could not generate derivatives with DS(Ac) > 2.81 and DS(Br) < 0.19, we investigated the effect of adding Ac_2O before NBS and PPh_3. Since the C6 primary alcohol of polysaccharides is observed to be the most reactive towards acylation (Xu, Li, Tate, & Edgar, 2011), we hoped that we could acetylate some primary hydroxyls before conducting bromination, reducing the available C6-OH that could be brominated. This approach proved successful; we obtained DS(Ac) 2.96 and DS(Br) 0.04 after treatment with 10 eq per AGU of Ac_2O at room temperature for 2 h before adding brominating agents and increasing heat. The ^{13}C NMR spectrum for 2,3Ac-6Br amylose with DS(Ac) 2.96 and DS(Br) 0.04 is provided in Fig. 2. This further supports our belief that bromination and acylation are orthogonal reactions, as both C6-OAc and C6-Br are generated regardless of the order of reagent addition.

3.2. Synthesis of 2,3Ac-6N_3 amylose

Addition of a primary alkyl bromide at the C6-position incorporates a good leaving group for S_N2 displacement chemistry. The azide anion is a strong nucleophile that can quantitatively displace good leaving groups of functionalized polysaccharides, including tosylate (Liebert et al., 2006), chloride (Gao, Liu, & Edgar, 2018), and bromide moieties (Fox & Edgar, 2012). Similarly, treatment of 2,3Ac-6Br amylose with NaN_3 in DMSO at 80 °C for 24 h resulted in complete disappearance of the C6-Br resonance at 34.8 ppm in $CDCl_3$, replaced by a new resonance at 50.9 ppm attributed to the newly formed C6-N_3 group (Fig. 3). The resonance associated with C6-OAc methylene carbon remained unchanged at 62.2 ppm after azide substitution. There was no observed decrease in DS(Ac), indicating only S_N2 bromide displacement and no observable deacetylation. Additionally, there were no changes in chemical shifts of resonances associated with the acetyl methyl, acetyl carbonyl, and remaining AGU carbons in ^{13}C NMR, indicating selectivity only for bromide substitution. The doublet resonances associated with the C6-Br methylene protons from 3.67 to 3.77 ppm disappeared as a new signal appeared from 3.50 to 3.62 ppm, attributed to C6-N_3 methylene protons (see Supplementary Information).

Azide incorporation was also confirmed by FTIR. An absorption band is present at 2103 cm^{-1} (Fig. 4), attributed to the azide stretching mode. The relative intensity of the azide absorption band compared to the carbonyl absorption band at 1744 cm^{-1} and the acetyl methyl symmetric bending mode at 1371 cm^{-1} decreased with increasing DS(Ac), due to concomitant increase of DS(Ac) with decreasing DS(N_3). There was no observable -OH stretching band, indicating complete substitution and no deacetylation during azide substitution, in agreement with DS(Ac) results obtained from ^1H NMR.

3.3. CuAAC of 2,3Ac-6N_3 amylose with TBPE: Synthesis of 2,3Ac-6tBu amylose

We chose TBPE as our alkyne click partner in part due to the well-

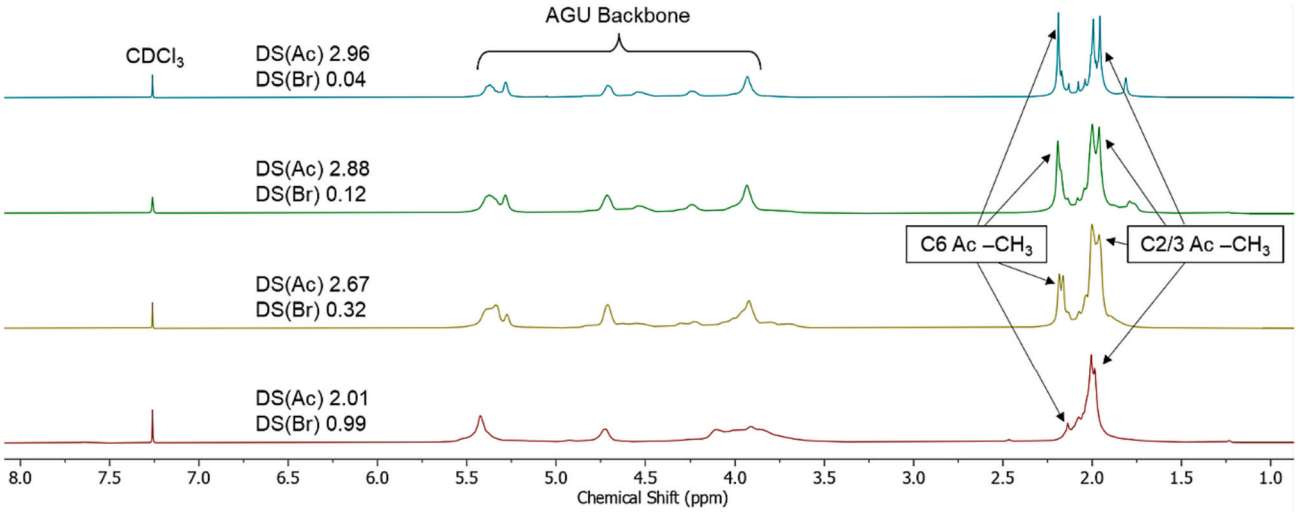

Fig. 1. Stacked ^{1}H NMR spectra of 2,3Ac-6Br amyloses with varying DS(Ac)/DS(Br).

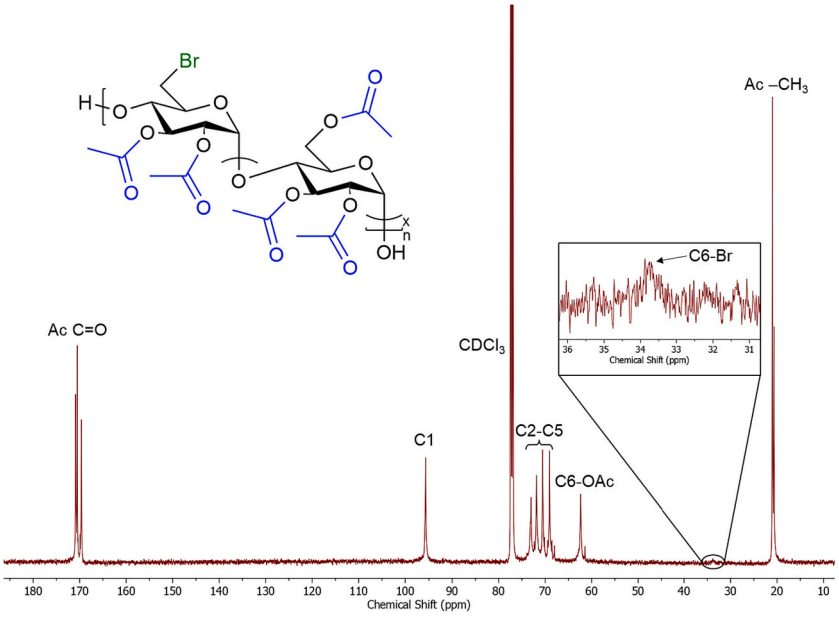

Fig. 2. ^{13}C NMR spectrum of 2,3Ac-6Br amylose DS(Ac) 2.96/DS(Br) 0.04.

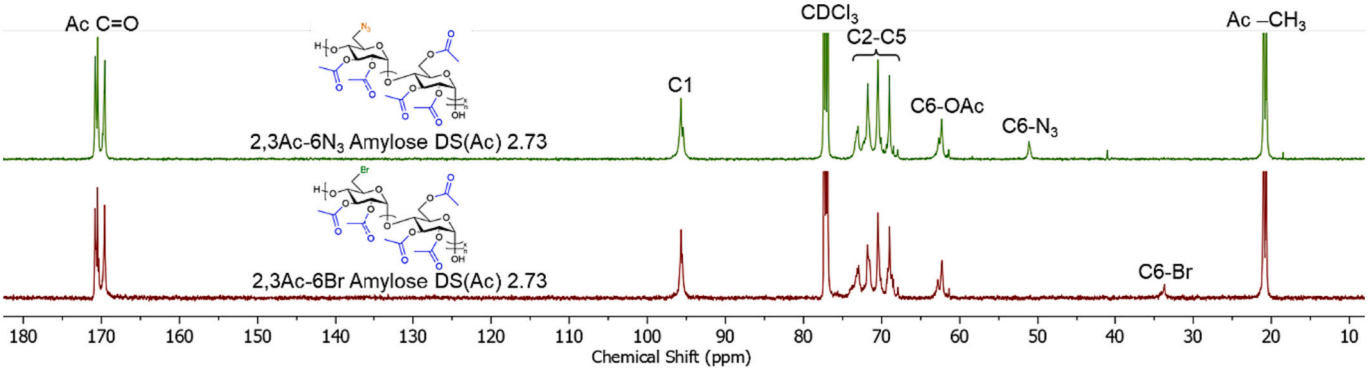

Fig. 3. Stacked ^{13}C NMR spectra of 2,3Ac-6Br and 2,3Ac-6N_3 amyloses with DS(Ac) 2.73.

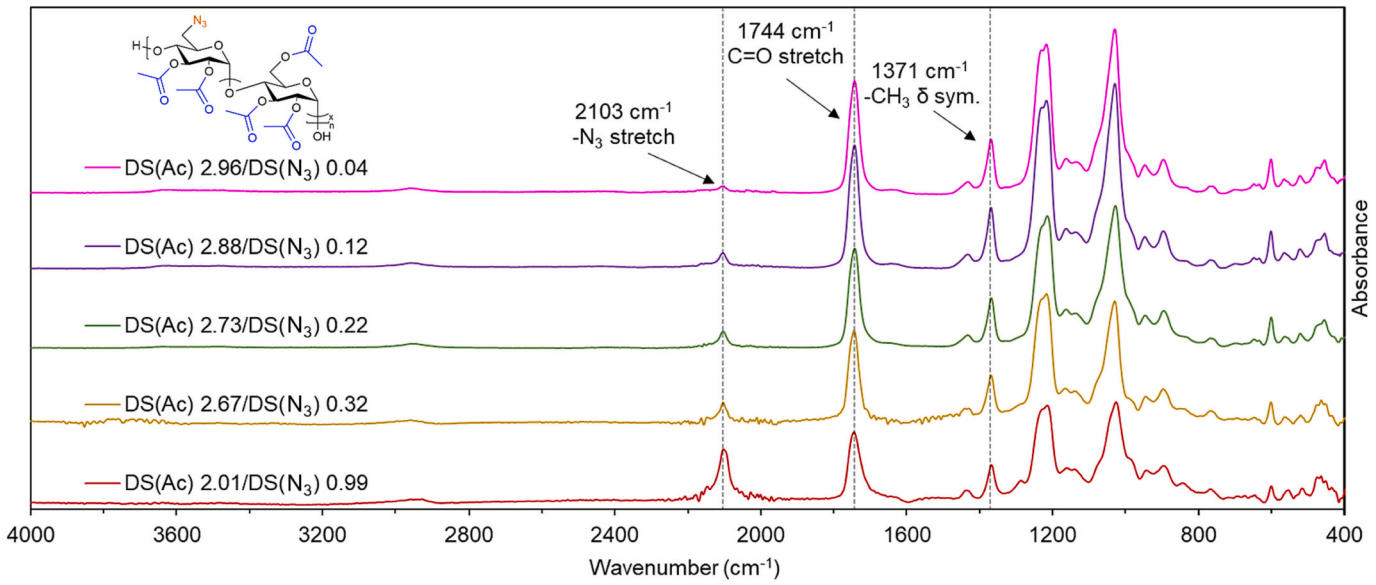

Fig. 4. Stacked FTIR spectra of 2,3Ac-6N_3 amyloses with varying DS(Ac)/DS(N_3).

resolved *tert*-butyl ^{1}H resonance near 1.20 ppm that could be easily analyzed to check DS(*t*Bu), which also sets the minima for DS(N_3) and DS(Br), since CuAAC depends first on bromination, then azidation (both azide displacement and CuAAC are typically quantitative reactions). Treatment of 2,3Ac-6N_3 amylose DS(Ac) 2.01 with a slight excess of TBPE and a catalytic amount of Cu(I)Br and PMDETA in DMF resulted in the formation of the 1,2,3-triazole at the C6 position. This was confirmed by ^{1}H NMR spectroscopy, with the appearance of new singlet resonances at 1.19 and 7.84 ppm in 1:1 $CDCl_3$:DMSO-d_6, attributed to the *tert*-butyl methyl and triazole methine protons, respectively, as shown in Fig. 5.

Successful CuAAC was further confirmed by the appearance of new ^{13}C NMR resonances at 27.3, 55.4, 73.1, 125.1, and 145.3 ppm, corresponding to the *tert*-butyl methyl, TBPE methylene, *tert*-butyl quaternary, tertiary triazole, and quaternary triazole carbons, respectively (See Supplementary Information). The chemical shift in ^{13}C NMR associated with C6-*N*- moved from 50.9 to 49.5 ppm after CuAAC. As seen in Fig. 6, the HSQC spectrum of 2,3Ac-6*t*Bu amylose DS(Ac) 2.01/DS(*t*Bu) 0.99 exhibits a correlation at 7.95 and 124.7 ppm in DMSO-d_6, corresponding to the triazole methine proton formed after CuAAC. Comparing the HSQC spectrum of 2,3Ac-6N_3 amylose DS(Ac) 2.01 in DMSO-d_6 to that of 2,3Ac-6*t*Bu shows that the ^{1}H NMR resonances of the C4 and C5 methine protons changed appreciably. The C4 methine proton shifted downfield from 3.95 to 4.22 ppm while the C5 methine proton shifted upfield from 3.94 to 3.51 ppm after CuAAC (See Supplementary Information).

For 2,3Ac-6*t*Bu amylose, the ^{13}C resonances associated with the *tert*-butyl and triazole carbons were significantly sharper compared to those of the AGU repeat unit (see Supplementary Information). Narrower line widths in NMR spectra indicate a longer T_2 relaxation (i.e., spin-spin relaxation) time, which is indicative of higher molecular mobility (Ablett, Clark, & Rees, 1982). This decrease in line widths is indicitave of higher mobility for the triazole and *tert*-butyl groups, due to their separation from the less mobile amylose backbone. A similar difference in line widths in ^{13}C NMR between the polysaccharide backbone and moieties regioselectively appended at the C6-position was observed for amino acid ester conjugates of cellulose acetate (Zhou & Edgar, 2022).

Further confirmation of successful Huisgen click reaction was provided by FTIR spectroscopy. The azide stretching band at 2103 cm^{-1} completely disappeared after CuAAC of 2,3Ac-6N_3 amylose with TBPE, supporting complete conversion to triazole (Fig. 7). A new band appeared at 1711 cm^{-1} next to the carbonyl absorption band at 1744 cm^{-1}, which is attributed to the stretching mode of the triazole alkene. Another band at 2973 cm^{-1} is attributed to the stretching mode of the

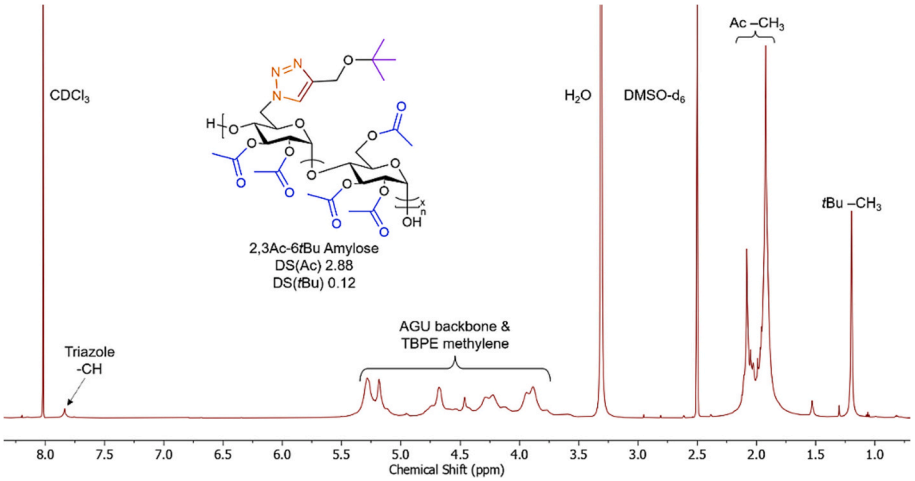

Fig. 5. ^{1}H NMR spectrum of 2,3Ac-6*t*Bu amylose DS(Ac) 2.88/DS(*t*Bu) 0.12.

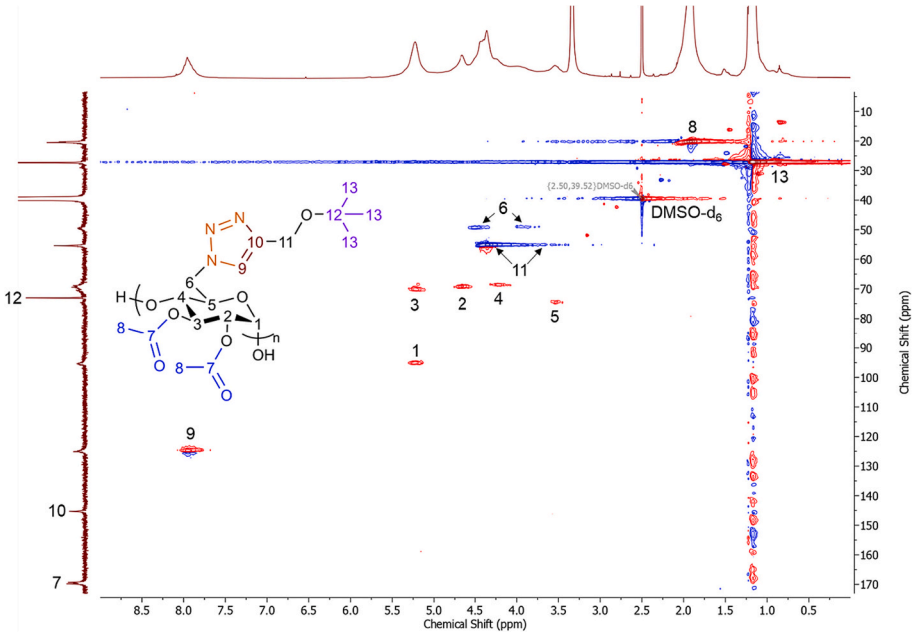

Fig. 6. HSQC NMR spectrum of 2,3Ac-6*t*Bu amylose with DS(Ac) 2.01/DS(*t*Bu) 0.99.

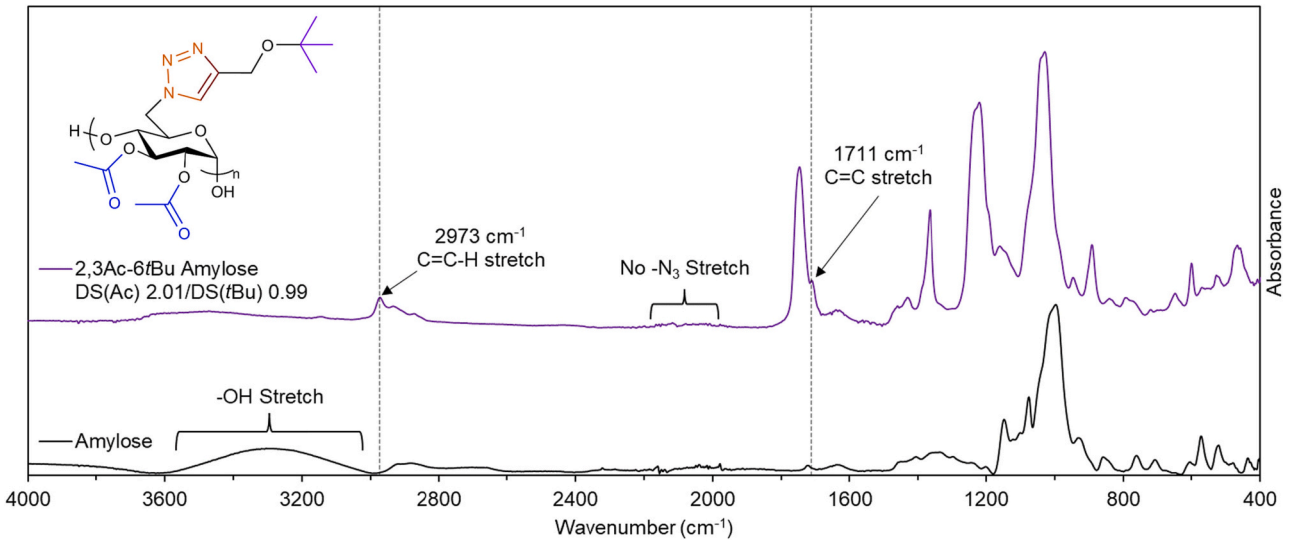

Fig. 7. Stacked FTIR spectra of amylose and 2,3Ac-6*t*Bu amylose DS(Ac) 2.01/DS(*t*Bu) 0.99.

Table 2
DS(N_3) as calculated from EA, $q^{13}C$ NMR, and ^1H NMR of CuAAC product with TBPE.

Entry	DS(Ac) (^1H NMR)	DS(N_3) (EA)	DS(N_3) ($q^{13}C$ NMR)	DS(*t*Bu) (^1H NMR)
A	2.01	0.97	0.99	0.99
B	2.64	0.36	0.38	0.35
C	2.67	0.36	0.37	0.32
D	2.73	0.25	0.26	0.22
E	2.81	0.17	0.19	0.17
F	2.71	0.29	0.29	0.28
G	2.68	0.23	0.24	0.25
H	2.88	0.16	0.14	0.12
I	2.96	0.06	0.05	0.04

triazole alkene methine proton. Absence of the broad amylose-OH stretching band centered at 3305 cm^{-1} indicates that almost all hydroxyl groups were functionalized and that there was no observable deacetylation during CuAAC. As shown in Table 2, we had good agreement between DS(*t*Bu) obtained from ^1H NMR and DS(N_3) obtained from both EA and $q^{13}C$ NMR spectroscopy. All derivatives had DS (OH) $\leq$ 0.07 (calculated by difference, DS(OH) = 3 – DS(Ac) – DS(other C-6 substituent) according to ^1H NMR), indicating that almost all hydroxyl groups had been transformed into acetate esters or bromide moieties in the first step, consistent with FTIR results noted above.

3.4. Thermal properties and molecular weight analysis of regioselectively functionalized amylose acetates

Thermal properties of polysaccharide derivatives, including both glass transition temperatures (T_g) and thermal decomposition behavior, depend not only on the composition of substituted positions but also on

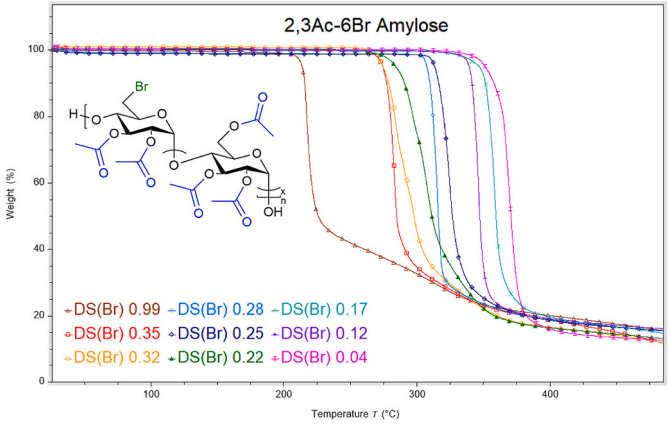

Fig. 8. TGA thermograms of 2,3Ac-6Br amyloses with varying DS(Ac)/DS(Br).

the position of substitution (Xu, Voiges, Elder, Mischnick, & Edgar, 2012). Each of the derivatives prepared had thermal behavior that depended both on the identity of the C6 substituent and DS(C6) (and in turn, DS(Ac)). For 2,3Ac-6Br amyloses, the onset temperature of thermal degradation, as observed with TGA, increased dramatically with an increase in DS(Ac) and decrease of DS(6-Br). As shown in Fig. 8, 2,3Ac-6Br amylose DS(Ac) 2.01 showed high thermal stability until 212 °C, after which there was a precipitous drop to approximately 45% of its starting mass. Similar thermal degradation behavior was observed for similarly prepared 2,3Ac-6Br cellulose (Fox & Edgar, 2011). While the exact mechanism of thermal decomposition of polysaccharide esters brominated at C-6 is not known, cellulose triacetate is known to thermally decompose via elimination of acetic acid (Scotney, 1972). We believe that part of this degradation behavior of 2,3Ac-6Br amylose can be rationalized by the thermal elimination of HBr which can catalyze both the elimination of acetic acid and hydrolysis of the glycosidic linkage. As DS(Br) decreases, less HBr would be available to be eliminated, requiring a higher amount of thermal energy to cause HBr-catalyzed degradation. The effects of azide substitution and CuAAC with TBPE on thermal stability were also observed with TGA. Degradation for 2,3Ac-6N_3 derivatives occurred at lower temperatures compared to the brominated derivatives, but exhibited a much slower loss in mass with increasing temperature. Similar results were observed for other azide-containing polymers, with the degradation mechanism attributed to the release of N_2 and formation of an alkyl nitrene (You, Kweon, Kang, & Noh, 2010). However, after CuAAC with TBPE, thermal stability was less dependent on DS(C6) and had decomposition onset temperatures that were higher than their corresponding 6-Br or 6-N_3 derivatives. The derivative which showed the highest thermal stability was 2,3Ac-6*t*Bu amylose DS(Ac) 2.96/DS(*t*Bu) 0.04 exhibiting an onset of thermal degradation at 365 °C (See Supplementary Information). In general, the onset of thermal degradation increased with DS(Ac) and decreasing DS (C6) for all derivatives.

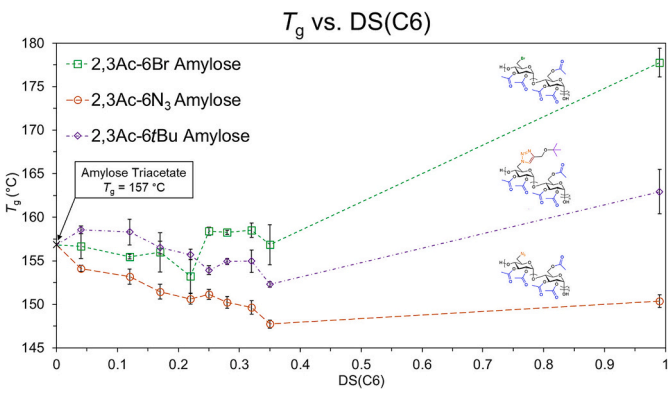

Fig. 9. T_g vs DS(C6) for regioselectively functionalized amylose acetates.

DSC analysis was conducted to investigate how T_g was affected by DS (Ac), DS(C6), and the composition at the C6 position. As shown in Fig. 9, T_g decreased with increasing DS(N_3), but increased with increasing DS (6-Br) and DS(6-*t*Bu). The highest T_g of 178 °C observed was for 2,3Ac-6Br DS(Ac) 2.01/DS(Br) 0.99, while the lowest T_g of 148 °C was observed for 2,3Ac-6N_3 DS(Ac) 2.64/DS(N_3) 0.35. The 2,3Ac-6N_3 derivatives consistently had the lowest T_g for all compositions, while the 2,3Ac-6Br derivatives had the highest T_g for derivatives with 2.01 < DS (Ac) < 2.71 and the 2,3Ac-6*t*Bu derivatives had the highest T_g for derivatives with DS(Ac) > 2.71.

These results indicate that both nature and DS of the C6 substituent impact polymer mobility and energy required to initiate cooperative segmental backbone motion characteristic of the glass transition. As DS (Ac) approaches 3.00 and DS(C6) approaches 0, the T_g of each derivative converges to the range of 154–159 °C, which suggests that the composition of the C6 position has less of an impact on molecular mobility as DS(C6) decreases. Amylose esters with DS(Ac) 2.50 (Shogren, 1996) and 2.70 (Fringant et al., 1996) exhibited T_g values at 165 and 150 °C, respectively. The amylose acetates with DS(Ac) > 2.97 that did not undergo bromination during the one-pot reaction of amylose in DMAc/LiBr exhibited a T_g of 157 °C, which is within the range of T_g values for amylose acetates with DS(Ac) 2.96 and DS(C6) 0.04. These results support our belief that the T_g of regioselectively substituted amylose acetates approaches the T_g of amylose acetate DS(Ac) 3.00 as DS(C6) decreases and DS(Ac) increases, suggesting that the C6 substituent type and DS affect polymer backbone mobility. Typical DSC thermograms for amylose derivatives with DS(Ac) 2.64/DS(C6) 0.35 are provided in Fig. 10.

Unexpectedly, we observed no distinct cold-crystallization exotherms or melting endotherms in any of the heating scans for any derivative, indicating that these derivatives are entirely amorphous. This is particularly surprising for derivatives with DS(Ac) 2.01 and 2.96, which are essentially homopolymers consisting of 2,3Ac-6X AGU or triacetyl AGU repeating units, respectively. Amylose triacetate is polymorphic with two distinct crystal structures: either a 14/3 helix for amylose triacetate I or a 9/7 helix for amylose triacetate II (Takahashi & Nishikawa, 2003). We would expect that the low DS(C6-X) for these derivatives would not inhibit crystallization, as there should be stretches of amylose triacetate segments that are long enough (approximately 25 repeat units on average) to crystallize into either polymorph I or polymorph II, containing 14 and 9 repeat units per crystalline unit cell, respectively. It is possible that these materials are semicrystalline but that melting transitions occur after thermal decomposition, similar to cellulose triacetate (Sata, Murayama, & Shimamoto, 2004) and *O*-acylated-6-deoxy-6-bromocellulose (Fox & Edgar, 2011).

While the regioselectivity of functionalization at the C6 is well-controlled due to the selective nature of the chemical modifications employed, there is no control over the sequence distribution of functionalized C6 moieties along each polysaccharide chain. As a result, each derivative can be considered as a random copolymer consisting of two repeating units: the 2,3,6Ac AGU repeat unit and the 2,3Ac-6X AGU repeat unit. Assuming that the triacetylated and regioselectively-functionalized repeat units are miscible, the dependence of T_g on DS (C6) should have a linear dependence governed by the weight fraction of each component repeat unit described by the Fox equation. Deviations from the Fox equation are typically indicative of specific inter- and intramolecular interactions arising from sequence distribution and steric effects (Lee & Litt, 2000). Although we have not investigated in detail the exact cause of this non-linear dependence of T_g on DS(C6), it should be an important consideration when designing well-defined amylose acetate derivatives for future structure-property relationship studies, such as the regioselective synthesis of well-defined amylose-based graft polymers.

Molecular weight (MW) determination of each derivative was

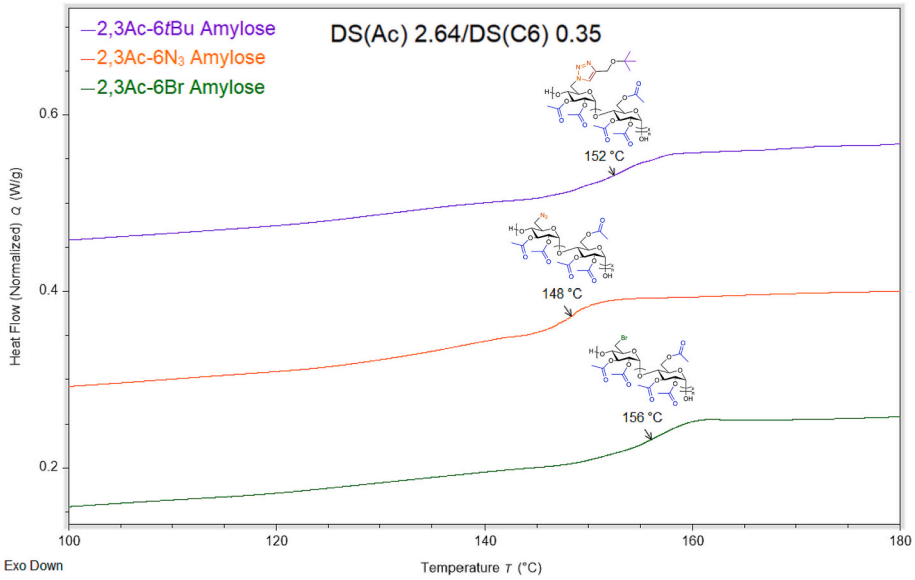

Fig. 10. Typical DSC thermograms for amylose derivatives with DS(Ac) 2.64/DS(C6) 0.35.

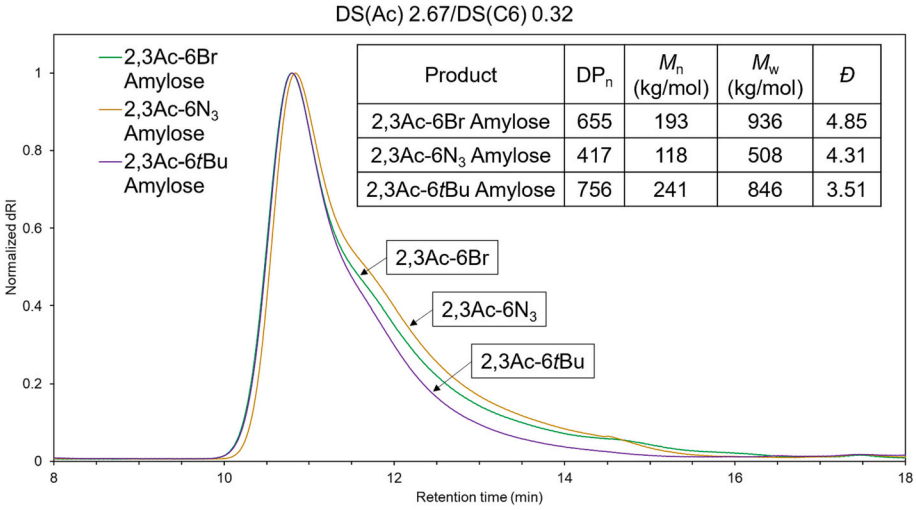

Product	DP_n	M_n (kg/mol)	M_w (kg/mol)	$Đ$
2,3Ac-6Br Amylose	655	193	936	4.85
2,3Ac-6N$_3$ Amylose	417	118	508	4.31
2,3Ac-6*t*Bu Amylose	756	241	846	3.51

Fig. 11. SEC chromatograms for regioselectively functionalized amylose derivatives with DS(Ac) 2.67/DS(C6) 0.32.

conducted using SEC. All derivatives were soluble in DMAc with 50 mM LiCl, although some product solutions could not be filtered before SEC analysis, preventing MW determination. A representative SEC chromatogram for amylose derivatives with DS(Ac) 2.67/DS(C6) 0.32 is provided in Fig. 11.

In general, DP decreased during the bromination/acetylation and azide substitution steps, but appeared to increase after CuAAC. The DP loss during the bromination/acetylation step could be attributed to acid-catalyzed hydrolysis of glycosidic linkages of the amylose backbone due to the generation of acetic acid during the reaction. Dissolution of polysaccharides in DMAc solvent systems has also been observed to reduce DP, likely due to the formation of *N,N*-dimethylketeniminum salts which can cleave acetals along the polysaccharide backbone (Potthast, Rosenau, Sixta, & Kosma, 2002). Therefore, the DP loss from the synthesis of 2,3Ac-6Br amylose could be a result of backbone degradation during both the dissolution and functionalization steps. Further DP loss was also observed after azide substitution in DMSO, as the chromatogram for 2,3Ac-6N$_3$ amylose DS(Ac) 2.67 shifted to later retention times compared to the chromatogram for 2,3Ac-6Br amylose DS(Ac) 2.67, indicating a decrease in MW. Similar DP loss was also observed for the azide substitution of 6-bromo-6-deoxycellulose (Fox & Edgar, 2012) and 6-bromo-6-deoxypullulan (Pereira & Edgar, 2014) acetates. Interestingly, the SEC chromatogram for 2,3Ac-6*t*Bu amylose DS(Ac) 2.67 shifted to earlier retention times compared to 2,3Ac-6N$_3$ amylose DS (Ac) 2.67, indicating an increase in MW and an apparent increase in DP. This could indicate aggregation during SEC, although there were no instances of a strong light scattering without a corresponding RI signal, indicative of aggregation (Pereira & Edgar, 2014). We hypothesize that the increase in DP could be a result of steric bulk of the appended triazole and *tert*-butyl moieties, which may result in a more extended conformation in solution, resulting in an artificially increased DP as obtained from light scattering. It is also possible that low MW fractions of amylose derivatives were removed during the multiple precipitations that occurred during workup after each reaction, which would inflate DP. It should also be noted that the MW reported was determined via multi-angle light scattering, while the chromatogram provided is the dRI vs. retention time trace. The prepared amylose derivatives were near the limit of selective permeation for the columns employed (100 kg/mol), limiting resolution between dRI signals for high MW amylose derivatives. Regardless, the chromatograms provided indicated a shift

towards later retention times after azide substitution (indicating loss of MW) and a shift towards earlier retention times after CuAAC with TBPE (indicating increase of MW). As such, there is no direct evidence of DP loss as a result of main chain scission, suggesting that CuAAC is mild enough to preserve MW. It should also be noted that the calculations used to determine DP for regioselectively modified amylose esters can be complex due to the range of DS and presence of different substituents. Variations in DS and substituents could also affect polymer-solvent interactions, which may change the derivative's hydrodynamic radius in the eluent, which may alter the detected MW.

4. Conclusions

In summary, we have demonstrated efficient, one-pot synthesis of 2,3Ac-6Br amylose with control over DS(Br) and DS(Ac) through varying stoichiometry, reaction times, and order of reagent addition. DS(Ac) ranging from 2.01 to 2.81 was achieved through variation of NBS/PPh_3: AGU and bromination reaction time, while DS(Ac) $>$ 2.88 was only obtained by adding Ac_2O prior to the addition of NBS/PPh_3. Importantly, DS(Br) of $<$0.1 was achieved by this early Ac_2O addition method, enabling synthesis of a comb-like structure with "tines" at frequency just under 1 per 10 AGUs, which is very promising for future work on comb-like copolymers. Quantitative azide substitution generated a series of *O*-acetylated-6-azido-6-deoxyamyloses with DS(Ac) ranging from 2.01 to 2.96 and DS(N_3) ranging from 0.04 to 0.99. TBPE was employed as a model alkyne for CuAAC which allowed for the determination of DS(N_3) by ^{1}H NMR (using the assumption that CuAAC was quantitative; quantification of DS(*t*Bu) sets a minimum for DS(N_3) of the precursor). FTIR spectroscopy indicated full conversion of CuAAC for all compositions due to the complete disappearance of the azide stretching absorption band at 2103 cm^{-1}. Thermal stability depended heavily on both DS(Ac) and the composition of the C6-position, with thermal stability increasing with DS(Ac). DS(Ac) and the C6 moiety also affected T_g, with T_g converging to 154–159 °C as DS(Ac) approaches 3.00, which approaches the T_g of amylose triacetate.

Regioselectively substituted 2,3Ac-6N_3 amyloses with varying DS (N_3) will be used to generate well-defined comb-like graft polymers as compatibilizers for immiscible polymer blends, which are the focus of upcoming studies. While in this work we modified amylose, this approach should be applicable to any polysaccharide with repeating primary hydroxyl groups to generate regioselectively *O*-acylated-6-azido-6-deoxy derivatives as substrates for CuAAC, generating useful materials for applications, e.g. in sustainable plastics and drug delivery.

CRediT authorship contribution statement

Jeffrey E. Thompson: Writing – original draft, Methodology, Investigation, Formal analysis, Data curation, Conceptualization. **Kevin J. Edgar:** Writing – review & editing, Supervision, Conceptualization.

Declaration of competing interest

The authors declare that they have no known competing financial interests or personal relationships that could have appeared to influence the work reported in this paper.

Data availability

Data will be made available on request.

Acknowledgements

This work was supported primarily by the Institute for Critical Technology and Applied Science (ICTAS) at Virginia Tech. This work was partially supported by GlycoMIP, a National Science Foundation Materials Innovation Platform funded through Cooperative Agreement DMR-1933525. We thank the Macromolecules Innovation Institute (MII) for facility access and their partial support of this work. The authors thank Jared Baker for conducting SEC analyses.

Appendix A. Supplementary data

Supplementary data to this article can be found online at https://doi.org/10.1016/j.carbpol.2024.121885.

References

Ablett, S., Clark, A. H., & Rees, D. A. (1982). Assessment of the flexibilities of carbohydrate polymers by ^{1}H NMR relaxation and line shape analysis. *Macromolecules, 15*, 597–602. https://doi.org/10.1021/ma00230a075

Barsi, D., Borsacchi, S., Calucci, L., Tarantino, A., Pinzino, C., & Bertoldo, M. (2017). Tuning the functionalization degree of amylose and amylopectin with photochromic spiropyran by CuAAc reaction. *Polymer, 120*, 82–93. https://doi.org/10.1016/j.polymer.2017.05.046

Bertoldo, M., Zampano, G., La Terra, F., Villari, V., & Castelvetro, V. (2011). Amphiphilic amylose-*g*-poly(meth)acrylate copolymers through 'Click' onto grafting method. *Biomacromolecules, 12*, 388–398. https://doi.org/10.1021/bm101143q

Cimecioglu, A. L., Ball, D. H., Huang, S. H., & Kaplan, D. L. (1997). A direct regioselective route to 6-azido-6-deoxy polysaccharides under mild and homogeneous conditions. *Macromolecules, 30*, 155–156. https://doi.org/10.1021/ma961282j

Cimecioglu, A. L., Ball, D. H., Kaplan, D. L., & Huang, S. H. (1994). Preparation of amylose derivatives selectively modified at C-6. 6-amino-6-deoxyamylose. *Macromolecules, 27*, 2917–2922. https://doi.org/10.1021/ma00089a004

Edgar, K. J., Arnold, K. M., Blount, W. W., Lawniczak, J. E., & Lowman, D. W. (1995). Synthesis and properties of cellulose acetoacetates. *Macromolecules, 28*, 4122–4128. https://doi.org/10.1021/ma00116a011

Fox, S. C., & Edgar, K. J. (2011). Synthesis of regioselectively brominated cellulose esters and 6-cyano-6-deoxycellulose esters. *Cellulose, 18*, 1305–1314. https://doi.org/10.1007/s10570-011-9574-3

Fox, S. C., & Edgar, K. J. (2012). Staudinger reduction chemistry of cellulose: Synthesis of selectively *O*-acylated 6-amino-6-deoxy-cellulose. *Biomacromolecules, 13*, 992–1001. https://doi.org/10.1021/bm2017004

Fox, S. C., Li, B., Xu, D., & Edgar, K. J. (2011). Regioselective esterification and etherification of cellulose: A review. *Biomacromolecules, 12*, 1956–1972. https://doi.org/10.1021/bm200260d

Fringant, C., Desbrières, J., & Rinaudo, M. (1996). Physical properties of acetylated starch-based materials: relation with their molecular characteristics. *Polymer, 37*, 2663–2673. https://doi.org/10.1016/0032-3861(96)87626-9

Furuhata, K., Koganei, K., Chang, H., Aoki, N., & Sakamoto, M. (1992). Dissolution of cellulose in lithium bromide-organic solvent systems and homogeneous bromination of cellulose with *N*-bromosuccinimide-triphenylphosphine in lithium bromide-*N,N*-dimethylacetamide. *Carbohydr. Res., 230*, 165–177. https://doi.org/10.1016/S0008-6215(00)90519-6

Gao, C., Liu, S., & Edgar, K. J. (2018). Regioselective chlorination of cellulose esters by methanesulfonyl chloride. *Carbohydr. Polym., 193*, 108–118. https://doi.org/10.1016/j.carbpol.2018.03.093

Huisgen, R. (1961). 1,3-Dipolar cycloadditions. *Proc. Chem. Soc.*, 357–396. https://doi.org/10.1039/PS9610000357

Imre, B., Kiss, E. Z., Domján Cui, L., & Pukánszky, B. (2021). Ring-opening polymerization of ε-caprolactone from cellulose acetate by reactive processing. *Cellulose, 28*, 9103–9116. https://doi.org/10.1007/s10570-021-04038-8

Jiang, F., Wang, Z., Qiao, Y., Wang, Z., & Tang, C. (2013). A novel architecture toward third-generation thermoplastic elastomers by a grafting strategy. *Macromolecules, 46*, 4772–4780. https://doi.org/10.1021/ma4007472

Kamitakahara, H., Enomoto, Y., Hasegawa, C., & Nakatsubo, H. (2005). Synthesis of diblock copolymers with cellulose derivatives. 2. Characterization and thermal properties of cellulose triacetate-block-oligoamide-15. *Cellulose, 12*, 527–541. https://doi.org/10.1007/s10570-005-7135-3

Karan, H., Funk, C., Grabert, M., Oey, M., & Hankamer, B. (2019). Green bioplastics as part of a circular bioeconomy. *Trends Plant Sci., 24*, 237–249. https://doi.org/10.1016/j.tplants.2018.11.010

Kilmovica, K., Pan, S., Lin, T., Peng, X., Ellison, C. J., LaPointe, A. M., … Coates, G. W. (2020). Compatibilization of *i*PP/HDPE blends with PE-*g*-*i*PP graft copolymers. *ACS Macro Lett., 9*, 1161–1166. https://doi.org/10.1021/acsmacrolett.0c00339

Kinose, Y., Sakakibara, K., Ogawa, H., & Tsujii, Y. (2019). Main-chain stiffness of cellulosic bottlebrushes with polystyrene side chains introduced regioselectively at the *O*-6 position. *Macromolecules, 52*, 8733–8740. https://doi.org/10.1021/acs.macromol.9b01628

Lee, J., & Litt, M. H. (2000). Glass transition temperature-composition relationship of oxyethylene copolymers with chloromethyl/(ethylthio)methyl, chloromethyl (ethylsulfinyl)methyl, or chloromethyl/(ethylsulfonyl)methyl side groups. *Polym. J., 32*, 228–233. https://doi.org/10.1295/polymj.32.228

Liebert, T., Hänsch, C., & Heinze, T. (2006). Click chemistry with polysaccharides. *Macromol. Rapid Commun., 27*, 208–213. https://doi.org/10.1002/marc.200500686

Liu, S., & Edgar, K. J. (2017). Water-soluble co-polyelectrolytes by selective modification of cellulose esters. *Carbohydr. Polym., 162*, 1–9. https://doi.org/10.1016/j.carbpol.2017.01.008

Liu, S., Gao, C., Mosquera-Giraldo, L. I., Taylor, L. S., & Edgar, K. J. (2018). Selective synthesis of curdlan ω-carboxyamides by Staudinger ylide nucleophilic ring-opening. *Carbohydr. Polym., 190*, 222–231. https://doi.org/10.1016/j.carbpol.2018.02.074

Liu, S., Liu, J., Esker, A. R., & Edgar, K. J. (2016). An efficient, regioselective pathway to cationic and zwitterionic *N*-heterocyclic cellulose ionomers. *Biomacromolecules, 17*, 503–513. https://doi.org/10.1021/acs.biomac.5b01416

López-Barrón, C. R., & Tsou, A. H. (2017). Strain hardening of polyethylene/polypropylene blends via interfacial reinforcement with poly(ethylene-*cb*-propylene) comb block copolymers. *Macromolecules, 50*, 2986–2995. https://doi.org/10.1021/acs.macromol.7b00264

Marks, J. A., Fox, S. C., & Edgar, K. J. (2016). Cellulosic polyelectrolytes: synthetic pathways to regioselectively substituted ammonium and phosphonium derivatives. *Cellulose, 23*, 1687–1704. https://doi.org/10.1021/acs.biomac.5b01416

Meng, X., & Edgar, K. J. (2016). 'Click' reactions in polysaccharide modification. *Prog. Polym. Sci., 53*, 52–85. https://doi.org/10.1016/j.progpolymsci.2015.07.006

Pereira, J. M., & Edgar, K. J. (2014). Regioselective synthesis of 6-amino- and 6-amido-6-deoxypullulans. *Cellulose, 21*, 2379–2396. https://doi.org/10.1016/j.carbpol.2017.01.008

Pierre-Antoine, F., François, B., & Rachida, Z. (2012). Crosslinked cellulose developed by CuAAC, a route to new materials. *Carbohydr. Res., 356*, 247–251. https://doi.org/10.1016/j.carres.2011.10.028

Potthast, A., Rosenau, T., Sixta, H., & Kosma, P. (2002). Degradation of cellulosic materials by heating in DMAc/LiCl. *Tetrahedron Lett., 43*, 7757–7759. https://doi.org/10.1016/S0040-4039(02)01767-7

Rostovtsev, V. V., Green, L. G., Fokin, V. V., & Sharpless, K. B. (2002). A stepwise Huisgen cycloaddition process: Copper(I)-catalyzed regioselective 'ligation' of azides and terminal alkynes. *Angew. Chem. Int. Ed., 41*, 2596–2598. https://doi.org/10.1002/1521-3773(20020715)41:14<2596::AID-ANIE2596>3.0.CO;2-4

Saadatmand, S., Edlund, U., & Albertsson, A. (2011). Compatibilizers of a purposefully designed graft copolymer for hydrolysate/PLLA blends. *Polymer, 52*, 4648–4655. https://doi.org/10.1016/j.polymer.2011.08.053

Sata, H., Murayama, M., & Shimamoto, S. (2004). 5.4 properties and applications of cellulose triacetate film. *Macromol. Symp., 208*, 323–333. https://doi.org/10.1002/masy.200450413

Schatz, C., Louget, S., Le Meins, J., & Lecommandoux, S. (2009). Polysaccharide-block-polypeptide copolymer vesicles: Towards synthetic viral capsids. *Angew. Chem. Int. Ed., 48*, 2572–2575. https://doi.org/10.1002/anie.200805895

Scotney, A. (1972). The thermal degradation of cellulose triacetate-III. The degradation mechanism. *Eur. Polym. J., 8*, 185–193. https://doi.org/10.1016/0014-3057(72)90094-8

Self, J. L., Zervoudakis, A. J., Peng, X., Lenart, W. R., Macosko, C. W., & Ellison, C. J. (2022). Linear, graft, and beyond: multiblock copolymers as next-Generation compatibilizers. *JACS Au, 2*, 310–321. https://doi.org/10.1021/jacsau.1c00500

Seung, D. (2020). Amylose in starch: Towards understanding of biosynthesis, structure and function. *New Phytologist, 228*, 1490–1504. https://doi.org/10.1111/nph.16858

Shogren, R. L. (1996). Preparation, thermal properties, and extrusion of high-amylose starch acetates. *Carbohydr. Polym., 29*, 57–62. https://doi.org/10.1016/0144-8617(95)00143-3

Takahashi, Y., & Nishikawa, S. (2003). Crystal structure of amylose triacetate I. *Macromolecules, 36*, 8656–8661. https://doi.org/10.1021/ma030288n

Tornøe, C. W., Christensen, C., & Meldal, M. (2002). Peptidotriazoles on solid phase: [1,2,3]-triazoles by regiospecific copper(I)-catalyzed 1,3-dipolar cycloadditions of terminal alkynes to azides. *J. Org. Chem., 67*, 3057–3064. https://doi.org/10.1021/jo011148j

Tsou, A. H., López-Barrón, C. R., Jiang, P., Crowther, D. J., & Zeng, Y. (2016). Bimodal poly(ethylene-cb-propylene) comb block copolymers from serial reactors: Synthesis and applications as processability additives and blend compatibilizers. *Polymer, 104*, 72–82. https://doi.org/10.1016/j.polymer.2016.09.088

Xu, D., Li, B., Tate, C., & Edgar, K. J. (2011). Studies on regioselective acylation of cellulose with bulky acid chlorides. *Cellulose, 18*, 405–419. https://doi.org/10.1007/s10570-010-9476-9

Xu, D., Voiges, K., Elder, T., Mischnick, P., & Edgar, K. J. (2012). Regioselective synthesis of cellulose ester homopolymers. *Biomacromolecules, 13*, 2195–2201. https://doi.org/10.1021/bm3006209

Yamashita, E., Okubo, K., Negishi, K., & Hasegawa, T. (2009). Regioselective and quantitative modification of cellulose to access cellulose-based advanced materials: Cellulose-based glycoclusters. *Chem. Lett., 38*, 122–123. https://doi.org/10.1246/cl.2009.122

You, J., Kweon, J., Kang, S., & Noh, S. (2010). A kinetic study of thermal decomposition of glycidyl azide polymer (cap)-based energetic thermoplastic polyurethanes. *Macromol. Res., 18*, 1226–1232. https://doi.org/10.1007/s13233-010-1215-4

Zhang, R., & Edgar, K. J. (2014). Synthesis of curdlan derivatives regioselectively modified at C-6: *O*-(*N*)-Acylated 6-amino-6-deoxycurdlan. *Carbohydr. Polym., 105*, 161–168. https://doi.org/10.1016/j.carbpol.2014.01.045

Zhang, R., Liu, S., & Edgar, K. J. (2017). Efficient synthesis of secondary amines by reductive amination of curdlan Staudinger ylides. *Carbohydr. Polym., 171*, 1–8. https://doi.org/10.1016/j.carbpol.2017.04.093

Zhang, Y., Zhang, S., Liu, J., Hao, J., He, B., & Bai, Z. (2020). Further insight for the synthesis of 6-amino-6-deoxy amylose. *J. Appl. Polym. Sci.*, 138. https://doi.org/10.1002/app.49623

Zhou, Y., & Edgar, K. J. (2022). Regioselective synthesis of polysaccharide-amino acid ester conjugates. *Carbohydr. Polym., 277*(118), 886. https://doi.org/10.1016/j.carbpol.2021.118886